RESEARCH ON HYDRAULIC DRIVE CHASSIS OF TOBACCO HARVESTER IN SOUTHERN HILLY AREA
/
针对南方丘陵地区的烟叶收获机液压驱动底盘研究

Ting GUO[1), Dandan ZHANG[2), Shuo LIN[3), Tao ZHANG[4), Mingduan LU*[5)
[1) Hunan Tobacco Company Chenzhou Branch, Chenzhou 423000, China
[2) Guangdong Tobacco Company Shaoguan Branch, Shaoguan 512000, China
[3) Anhui Tobacco Company Wannan Branch, Wannan 242500, China
[4) Hunan Tobacco Company Changde Branch, Changde 415000, China
[5) College of Engineering and Technology, Southwest University, Chongqing 400715, China
Tel: +86-19562226905; E-mail: d15512606935@163.com
DOI: https://doi.org/10.35633/inmateh-75-70

Keywords: *tobacco harvester, hydraulic drive, steering wheel control, chassis design*

ABSTRACT
In order to solve the problems of inconvenient operation and easy loss of control levers in traditional tracked harvesters, this paper designs a hydraulic-driven chassis based on steering wheel control, and the structure and working principle of the chassis are described. The parameters such as track grounding length and drive wheel diameter are calculated; the design of the hydraulic drive system of the chassis is completed, and the driving control strategy is proposed. The test results show that the maximum speed of the chassis is 0.79 m/s, the minimum turning radius is 766 mm, and the failure rate tobacco rod clamping in field tests is only 4.37%. This design meets the needs of field operations, with high operability, stability, and ability, providing theoretical and practical basis for the development of tracked tobacco leaf harvesters.

摘要
为解决传统履带式收获机底盘操控不便、操纵杆易失位等问题，本文设计了一种基于方向盘控制的液压驱动底盘，并阐述了底盘结构、工作原理。对履带接地长度、驱动轮直径等参数进行了计算；完成了底盘液压驱动系统的设计，并提出了行驶控制策略。试验结果表明，底盘最高速度为 0.79 m/s，最小转弯半径为 766 mm，田间试验烟杆夹持失败率仅为 4.37%。该设计满足田间作业需求，具备较高操控性、稳定性和适应性，为履带式烟叶收获机的发展提供了理论与实践依据。

INTRODUCTION
The tobacco industry occupies an important position in China's national economy *(Liu et al., 2024*), and the tobacco growing areas in China are mainly concentrated in 20 provinces and cities in the south (Tan et al., 2023). At present, the harvest of tobacco leaves mainly relies on manual labor, with high labor intensity, high cost and low operation efficiency, which restricts the rapid development of tobacco industry *(Xue et al., 2024; Zhou et al., 2024*). Therefore, the realization of mechanized tobacco harvesting is of great significance to the development of the industry.

Hydraulic crawler chassis is a key component of harvesting machinery *(Wang B et al., 2024; Xi et al., 2024*). Its outstanding advantages lie in strong traction and adaptability, low ground specific pressure, excellent obstacle crossing and load carrying capacity, and can work efficiently under complex conditions *(Pan et al., 2024; Xiao et al., 2024; Du et al., 2023*). By directly connecting the hydraulic pump and hydraulic motor, the hydraulic system eliminates transmission components such as transmission and differential, greatly improving transmission efficiency. Based on the growth characteristics of sweet sorghum, *Wu L et al., (2018*), designed a hydraulic driven harvester chassis, which uses dual pumps to drive the motor and can adjust the operation speed according to the density of plants. *Wang P et al., (2022*), designed 4CJZ-1000 self-propelled crawler tea picker. The crawler chassis controlled the power output of the gasoline engine through a pull-press joystick to realize movement and stopping. *Xiao Wenying et al.* (*2023*), designed a tractor hydraulic drive system and verified its applicability under large loads through field tests. *Li et al., (2024*), designed a fully hydraulic tracked power chassis, which uses a closed triple plunger pump to provide power for the driving and operating mechanism. *Wang et al., (2023*), designed a special chassis for the Chinese sugarcane harvester, and the hydraulic system realized the steering function by controlling the steering cylinder valve core.

At present, the variable pump displacement adjustment of most hydraulic systems is still achieved by turbine rack drive or joystick control valve, which has some problems such as inflexible control, out of position and unstable oil supply, which seriously affects the handling performance and safety of tracked vehicles.

Aiming at the above problems, a hydraulic driven tobacco leaf harvesting machine chassis is designed in this paper. The steering wheel control mechanism is used instead of the traditional joystick to realize the straight running and turning control of the chassis. Prototype production and performance verification were carried out to provide equipment support for tobacco leaf harvest in hilly and mountainous areas of South China.

MATERIALS AND METHODS

Structure of tobacco harvester

In order to meet the requirements for baking the upper leaf belt stalks after harvesting the lower leaves, the tobacco leaf harvester is primarily designed to perform two tasks: harvesting the upper leaves of the tobacco stalk and crushing the remaining stalk. The harvester consists of a chassis, control cabinet, soil excavation mechanism, clamping transmission mechanism, cutting mechanism, crushing and collection mechanism, guide collection mechanism, and collection box, as shown in Figure 1.

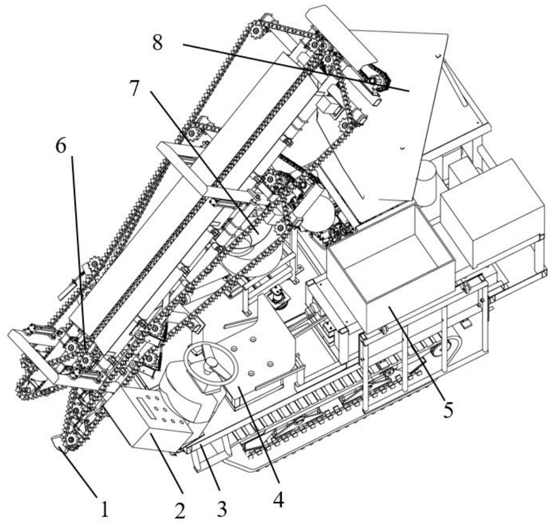

Fig. 1 - Schematic diagram of tobacco leaf harvester
1.Soil Loosening Mechanism; 2. Control Cabinet; 3. Rack; 4. Chassis; 5. Collection Box;
6. Clamping Conveying Mechanism; 7. Crushing Collection Mechanism; 8. Guiding Collection Mechanism

The tobacco harvester sequentially performs digging, conveying, cutting, crushing, and collecting of tobacco stalks. After starting the machine by pressing the control button on the control cabinet, the operator adjusts the position of the entire machine so that the tobacco stalks enter the feeding inlet of the clamping transmission mechanism. During operation, the stalks are excavated and pulled upward, moving backward and upward along the clamping chain. When the stalks reach the feed inlet of the crushing mechanism, the cutting mechanism separates the upper stalk (with leaves) from the lower root. The lower root falls into the crusher for crushing, while the upper stalk carrying the tobacco leaves continues to move backward and upward along the clamping chain. The staff on the platform assist in collecting the falling tobacco leaves and guide them into the collection box via the guide bend plate, completing the harvesting process.

Hydraulic drive chassis structure of tobacco leaf harvester

The hydraulic drive chassis structure of the tobacco leaf harvester is shown in Figure 2. The chassis is powered by a diesel engine, and the engine's output is distributed in two ways via a transfer box: one output is connected to a series variable piston pump to drive the tracked chassis for movement and steering; the other is connected to a gear pump to power the operational mechanisms. The output shaft of the travel hydraulic motor is directly coupled to the drive wheel, eliminating traditional transmission components such as the gearbox, clutch, and drive shaft. This design enables efficient power transmission and reduces energy loss. The vehicle body is also equipped with a complete power supply system, hydraulic oil tank, diesel tank, hydraulic seat valve, radiator, and a steering wheel control system.

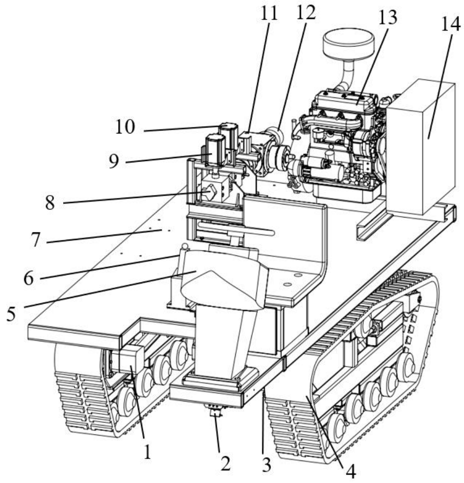

Fig. 2 - Schematic diagram of hydraulic drive chassis structure of tobacco harvester
1. Hydraulic motor K1; 2. Angle encoder; 3. Hydraulic motor K2; 4. Track device; 5. Steering wheel; 6. Shift handle; 7. Frame; 8. Series variable piston pump; 9. Stepper motor K1; 10. Stepper motor K2; 11. Transfer box; 12. Gear pump; 13. Engine; 14. Fuel tank

Working principle of hydraulic drive chassis

The chassis of the tobacco harvester is hydraulically driven, powered by a diesel engine and a series variable piston pump. The series variable piston pump in this system is equipped with two valves and is connected to the stepper motors K1 and K2 by coupling. When operating the steering wheel, the Angle encoder monitors the steering Angle in real time and feeds the signal back to the STM32 microcontroller. According to the received Angle signal, the MCU controls the stepper motor to rotate at a predetermined Angle, thus adjusting the opening of the two valves of the plunger pump. The valve can be rotated to neutral, forward, or reverse positions. When the valve is in the neutral position, the hydraulic oil flows directly back to the tank. When the valve is shifted to the forward or reverse position, the direction of the hydraulic oil flow changes accordingly, thereby controlling the forward or reverse rotation of the hydraulic motor. The size of the valve opening determines the speed of the hydraulic motor, so as to achieve the forward, backward and steering of the tobacco harvester chassis. In addition, through the shift lever, the driver can switch between different gear positions to achieve high, medium and low speed conversion. The outline of the series variable piston pump is shown in Figure 3, and the overall technical parameters of the chassis are shown in Table 1.

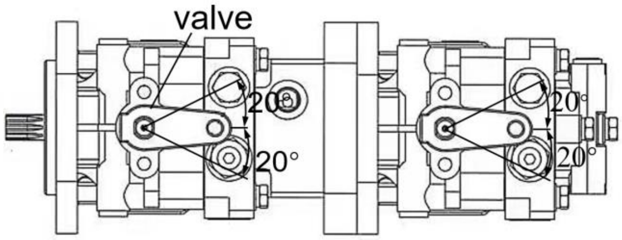

Fig. 3 - Outline of series variable piston pump

Table 1

Design parameters of hydraulic drive chassis of tobacco leaf harvester

Parameters	Numerical value
Dimensions (Length × Width × Height) / mm	1500×3000×2500
Travel mode	Crawler type
Crawler width / mm	230
Crawler ground contact length / mm	1300
Full load weight / kg	2000
Engine power / kW	31
Steering method	Differential steering
Track gauge / mm	1200

Calculation of track parameter

Compared with the wheeled device, the crawler chassis shows better stability, obstacle crossing ability and smaller ground specific pressure when facing the undulating road surface and complex working environment. Therefore, the crawler type traveling device is selected and its key parameters are calculated.

The ratio of track grounding length L to track gauge B has an important effect on the driving performance of the chassis. When the L/B value is large, steering becomes more difficult; When the L/B value is small, the driving stability will be reduced (*Wu et al., 2024; Chen et al., 2010*).

The empirical formula for calculating the track grounding length is shown in equation (1):

$$L=\left(1.15\sim1.39\right)B \tag{1}$$

where L is the grounding length of the track, [mm]; B is the gauge, [mm].

The value range of the ratio of track width to ground length is shown in equation (2):

$$0.18<\frac{b}{L}<0.24 \tag{2}$$

where b is the width of the track, [mm].

The drive wheel diameter is calculated using the following formula:

$$D=\frac{t}{\sin(\pi/n)} \tag{3}$$

where D is the diameter of the drive wheel, [mm]; t is the track pitch, [mm]; n is the number of teeth on the drive wheel.

To ensure no rolling damage to the ridge body in tobacco fields, appropriately increasing the track width helps reduce ground pressure and enhances traction and adhesion performance (*Ding et al., 2020; Li Qingjiang et al., 2024*). Based on calculations and available market track specifications, the track grounding length was determined to be 1300 mm, the width 230 mm, and the pitch 72 mm. The diameter of the drive wheel is 270 mm.

Principle of hydraulic system

The chassis of the crawler tobacco harvester adopts a double pump (series variable piston pump) double motor drive scheme, and each hydraulic pump controls a hydraulic motor to drive a single track. In this way, the track can be independently driven on both sides, and the hydraulic oil circuits on both sides are independent of each other, effectively avoiding the interference and coupling phenomenon between the systems. Its single-side track hydraulic system is shown in Figure 4, and the engine drives a series variable plunger pump to provide pressure oil, converting the mechanical energy into the pressure energy of the hydraulic oil. The pressure oil rotates by driving the hydraulic motor, thus driving the movement of the track driving mechanism. The hydraulic system adopts volumetric speed regulation technology, which has high working efficiency and good load adaptability. The traveling hydraulic motor is a bidirectional variable motor, and the speed and rotation direction of the hydraulic motor can be controlled by adjusting the valve opening and direction of the plunger pump. The safety relief valve in the system plays a load protection role to ensure that the working pressure of the hydraulic system is always maintained within the safe range. Finally, the hydraulic oil flows through the loop back to the radiator for cooling and then back to the tank.

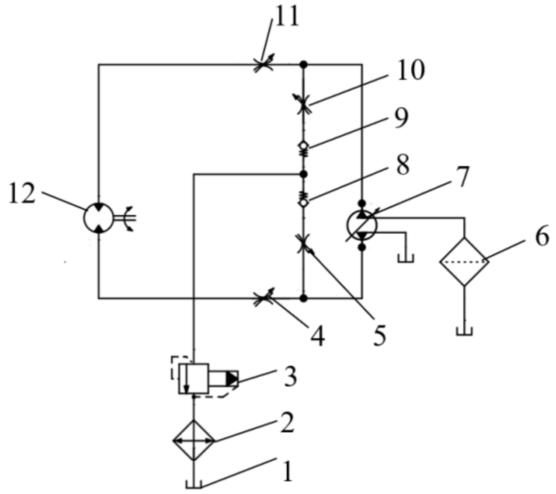

Fig. 4 - Schematic diagram of single-side pump-controlled hydraulic motor system

1.Fuel tank; 2. Air cooling; 3. Relief valve; 4, 5, 10, 11. Speed control valve;
6. Filter; 7. Plunger pump; 8, 9. Check valve; 12. Hydraulic motor

Selection of hydraulic motor

In the process of tobacco field operation, the chassis has the greatest resistance when running on the ramp, which mainly includes rolling resistance, slope resistance and acceleration resistance. In the tobacco leaf harvest operation, because the chassis is usually in a uniform motion state, the influence of acceleration resistance can be ignored. Therefore, the formula for calculating slope resistance is as follows:

$$F_a = Mgf\cos\alpha + Mg\sin\alpha \tag{4}$$

where F_a is the slope resistance, [N]; M is the mass of the whole machine, taken as 2000 kg; g is the acceleration of gravity, which is 9.8m/s^2; f is the operating resistance coefficient, which ranges from 0.08 to 0.12, and 0.12 is taken in this paper (*Mei et al., 2024*). α is the climbing angle, which is 20°.

The torque of the traveling hydraulic motor is shown in equation (5):

$$T = \frac{F_a r}{k\eta_1} \tag{5}$$

where T is the required torque of a single traveling hydraulic motor, [N·m]; r is the radius of the drive wheel, which is 0.134m; k is the number of traveling hydraulic motors, 2; η_1 is the efficiency of the track travel device, which is 0.9.

The theoretical displacement of traveling hydraulic motor is shown in equation (6):

$$V_c = \frac{2\pi T}{P\eta_2} \tag{6}$$

where V_c is the displacement of the traveling hydraulic motor, [ml/r]; P is the maximum working pressure of the hydraulic system, taking 15 MPa; η_2 is the mechanical efficiency of the traveling hydraulic motor and is taken as 0.9 (*Li et al., 2024*).

According to the driving speed of the chassis, the required speed of the hydraulic motor can be calculated, and the specific calculation formula is shown in equation (7):

$$n_c = \frac{1000v}{60\times 2\pi r} \tag{7}$$

where n_c is the maximum speed of the traveling hydraulic motor, [r/min]; v is the maximum driving speed of the chassis, which is 3 km/h.

By substituting the relevant design parameters into equations (4)~(7), it is calculated that the maximum resistance of the whole machine is 8914 N, the torque of a single traveling hydraulic motor is 664 N·m, the theoretical displacement is 309 ml/r, and the required speed is 60 r/min. Since the output shaft of the traveling hydraulic motor is directly connected to the drive wheel, the hydraulic motor needs to bear radial, axial and impact loads from the drive wheel (*Liu et al., 2022*), which puts higher requirements on the durability and torque capacity of the hydraulic motor. Therefore, after comprehensive evaluation, the BM5-400 hydraulic motor was finally selected. Its main technical parameters include: maximum displacement of 400 mL/r, output torque of 715 N·m, maximum output speed of 178 r/min, working pressure of 15 MPa, maximum input flow of 75 L/min.

Selection of hydraulic pump and engine

Hydraulic pump output flow is shown in equation (8):

$$Q_h = \frac{zKV_c n_c}{1000\eta_3} \tag{8}$$

where Q_h is the output flow rate of hydraulic pump, [L/min]; z is the number of hydraulic motors, taken as 2; K is the leakage coefficient of the hydraulic pump, taken as 1.1; η_3 is the volumetric efficiency of the traveling hydraulic motor, which is 0.9.

Hydraulic pump theoretical displacement is shown in equation (9):

$$V_h = \frac{1000Q_h}{n_h\eta_4} \tag{9}$$

where V_h is the theoretical displacement of hydraulic pump, ml/r; n_h is the speed of hydraulic pump, taken as 3000 r/min; η_4 is the volumetric efficiency of the hydraulic pump, which is 0.9.

By substituting the relevant parameters into equations (8) and (9), it is calculated that the output flow rate of the hydraulic pump is 46 L/min, and the theoretical displacement is 17 mL/r. According to the requirements of the system, two plunger pumps are installed in series, so the HAZE-21 series variable plunger pump is selected as the traveling hydraulic pump. The main technical parameters of the hydraulic pump include: maximum displacement of 21 mL/r, rated pressure of 17 MPa, rated speed of 3600 r/min. Each plunger pump will provide the required hydraulic energy for a traveling hydraulic motor.

According to the maximum flow required by the hydraulic system of the whole machine in the working process, the engine selection is further carried out. The calculation formula of engine power is as follows:

$$P_j = \frac{QP_h}{60\eta_5} \tag{10}$$

where P_j is the engine power, [KW]; Q is the required flow rate of the hydraulic system of the whole machine, [L/min]; P_h is the working pressure of the hydraulic pump, taken as 15 MPa; η_5 is the engine mechanical efficiency, which is 0.9.

The total flow required by the machine's hydraulic system is the sum of the flow demands of both the driving mechanism and the working mechanism. Based on calculations, the hydraulic system requires a flow rate of 100 L/min under maximum working conditions. According to Equation (10), the required engine power P_j is 28 kW. Taking into account engine size and output performance, the 4L22B diesel engine from Shandong Huayuan Laidong Internal Combustion Engine Co., Ltd. was selected. This engine provides a good performance match, with a rated power of 31 kW and a rated speed of 3300 r/min.

Control structure

The steering wheel operation mechanism is illustrated in Figure 5. When the steering wheel rotates, it drives the pinion via the steering shaft, with the pinion and large gear engaging through meshing teeth. A limiting gear mounted on the large gear restricts the pinion's rotation to one and a half turns in both directions, thereby limiting the steering wheel's total rotation range to ±540 degrees from the central position. As the steering wheel turns, the steering shaft and the angle encoder rotate synchronously, with the encoder capturing and transmitting the rotation angle data to the controller. The controller then calculates the required pulse count based on this angle data and adjusts the operation of stepper motors K1 and K2 accordingly. These stepper motors control the first and second flow control valves of the series variable piston pump, regulating the speed of hydraulic motors K1 and K2. The speed differential between the two motors enables the tracked vehicle to steer. The structure of the flow control valve mechanism is shown in Figure 6.

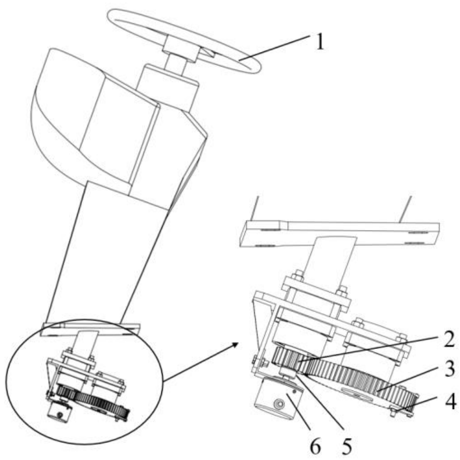

Fig. 5 - Structure diagram of steering wheel operating mechanism

1.Steering wheel; 2. Pinion; 3. Big gear; 4. Limit stop; 5. Steering shaft; 6. Angle encoder

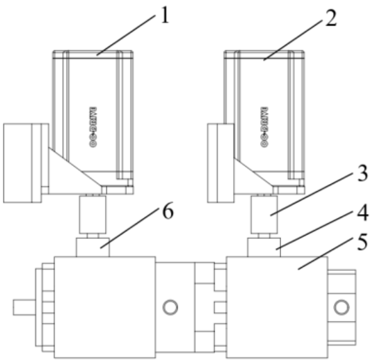

Fig. 6 - Flow control valve mechanism diagram

1.Stepping motor K1; 2. Stepping motor K2; 3. Coupling; 4. First class volume control valve;
5. Series variable piston pump; 6. Second flow control valve

Control System Integration

The steering wheel control system comprises a steering wheel, shift lever, stepper motors, and an angle encoder, as illustrated in Figure 7. The shift lever, adapted from an automotive automatic gear selector, includes five gear positions: forward fast (D3), forward medium (D2), forward slow (D1), park (P), and reverse (R). It is connected to the controller via five DuPont wires, transmitting five signals that enable the controller to synchronize the rotation angles of the two stepper motors. The angle encoder records the steering wheel's rotation angle and updates the rotation of the stepper motors accordingly. The system's controller is based on the STM32F103 core board, with the angle encoder connected through RS485 serial communication. A RS485-to-TTL chip is used to convert signals for compatibility. The controller's GPIO pins are linked to the motor driver board, which receives PWM pulse signals to control the stepper motors' movement. By adjusting the gear position and rotating the steering wheel, the chassis of the tobacco harvester can perform both linear and steering movements.

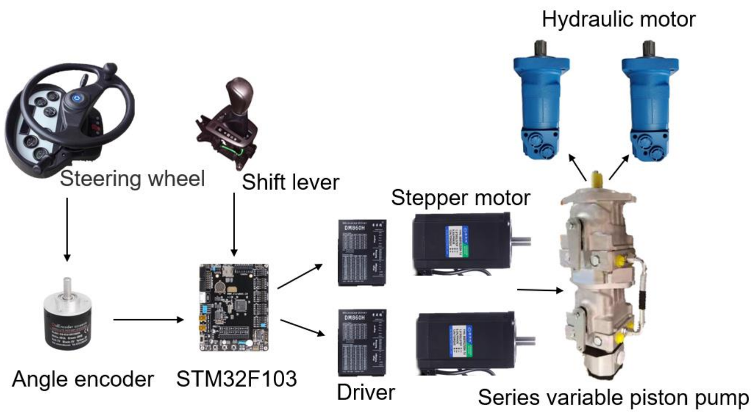

Fig. 7 - Schematic diagram of steering wheel system

Driving control strategy

(1) The controller determines the gear control signal of the straight-line operating mechanism:

The maximum rotation angle of the positive and negative direction of the flow control valve of the series variable piston pump is θ degree, and the number of pulses required by the rotation shaft of the motor to rotate 360 degrees is N, and the calculation formula is as follows:

$$N = \frac{360\partial}{\theta} \tag{11}$$

where θ is the step angle, measured in degrees; ∂ is a subdivision multiple and has no dimension.

The shift lever is equipped with n gears, each corresponding to a rotation angle α_n of the flow control valve (where n = 1, 2, 3, ..., and α $\alpha_n \leqq \theta$). Each gear position is associated with an external interrupt in the controller, and each external interrupt triggers a specific interrupt function. The number of pulses generated by the interrupt function is calculated using the formula: α_n*N/360.

According to the selected gear position, the controller simultaneously sends the corresponding number of pulses to both the first and second stepper motors. These two motors respectively control the first volume control valve and the second flow control valve to rotate to a predetermined angle. At this point, both hydraulic motors rotate in the same direction and at the same speed, thereby enabling the chassis to move in a straight line.

(2) After determining the gear position in step (1), the controller evaluates the steering signal from the steering wheel control mechanism:

Set the maximum steering wheel rotation angle in both clockwise and counterclockwise directions from the center (neutral) position to the limit stop as β. Let the angle γ be the current rotation angle of the steering wheel from the center position, as detected by the angle encoder, where $\gamma \leqq \beta$. For a given gear, the rotation angle of the flow control valve is α_n, corresponding to the steering wheel's rotation angle γ. Thus, for each 1° of steering wheel rotation from the center, the flow control valve must rotate by $\beta_n=2\alpha_n/\beta$.

When the steering wheel is turned clockwise by γ degrees, the stepper motor K1 remains stationary, and the controller commands the stepper motor K2 to rotate in the opposite direction by $|\gamma\beta_n|$ degrees. When the steering wheel is returned to its neutral position by γ degrees, the stepper motor K1 remains stationary, and the controller commands the stepper motor K2 to return to its original position by $|\gamma\beta_n|$ degrees;

When the steering wheel is turned counterclockwise by γ degrees, the stepper motor K2 remains stationary, and the controller commands the stepper motor K1 to rotate in the opposite direction by |γβn| degrees. When the steering wheel is returned to its neutral position by γ degrees, the stepper motor K1 remains stationary, and the controller commands the stepper motor K2 to return to its original position by |γβn| degrees.

By controlling the stepper motors K1 and K2, a speed difference is generated between the hydraulic motors K1 and K2, thereby controlling the steering of the track vehicle.

Analysis of steering performance

During operation, the steering system of the track chassis achieves directional control through differential movement. In the steering process, the tobacco harvester turns with a specific turning radius toward the side with the lower track speed. The diagram of differential steering is illustrated in Figure 8.

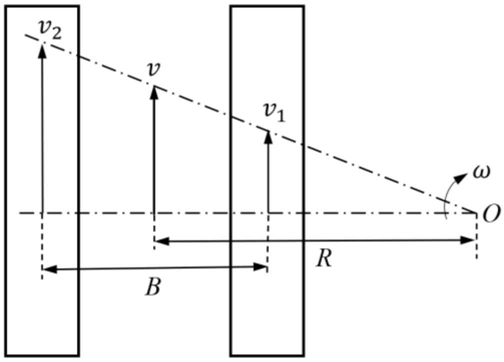

Fig. 8 - Diagram of differential right turn

Under ideal conditions, assuming that track slip and skid are negligible, the turning radius can be calculated using the following formula:

$$R=\frac{B(v_1+v_2)}{2(v_2-v_1)} \tag{12}$$

where R is the turning radius, [mm]; v_1 is the linear speed of the right track, [m/s]; v_2 is the linear speed of the left track, [m/s].

When the linear speeds of the right and left tracks are the same and in opposite directions, the tobacco harvester will achieve in-place turning of the chassis.

Test methods

The average plant spacing in the test field was approximately 400 cm, with row spacing ranging from 105 cm to 115 cm, and plant height ranging from 80 cm to 120 cm. The machine operated in slow gear mode, and three tobacco ridges were selected for harvesting, with each ridge having about 60 tobacco stalks. During the trial, the operation of the entire machine was observed, and the failure rate of tobacco stalk clamping for each ridge was calculated.

The calculation formula is as follows:

$$C = \frac{A_1}{A_2} \times 100\% \tag{13}$$

where C is the rate of tobacco rod clamping failure, [%]; A_1 is the number of tobacco rods not harvested in a single ridge; A_2 is the total number of tobacco rods in a single ridge.

RESULTS

Whole Machine Performance Test

The processing and trial production of the tobacco harvester chassis were completed at Guilin Maike Machinery Co., Ltd., and the upper working parts were successfully mounted. In order to comprehensively evaluate the performance and agronomic adaptability of the whole machine, performance tests were carried out in various aspects, mainly including driving speed test, steering performance test, and field harvesting effect test. The test instruments and equipment include tape measure, stopwatch, etc.

Driving Speed

The tobacco harvester is equipped with three forward speed gears, which are slow gear, medium gear, and fast gear, corresponding to the flow control valve rotation angles of 6 degrees, 12 degrees, and 20 degrees, respectively. The driving speed test was conducted according to the standard GB/T 10394.3-2002 "Feed Harvesters Part 3: Test Methods", as shown in Figure 9(a). The test selected a flat field road with a length of more than 50 meters. The driver, by operating the gear shift lever, used a stopwatch to measure the time required for the machine to travel 50 meters at the highest speed in a straight line at different gears. Each gear measurement was repeated 3 times and the average was taken, and then the highest driving speed at different gears was calculated. The test results are shown in Table 2.

(a) Driving speed

(b) Turning radius

Fig. 9 - Steering turning test

Table 2

Test results for driving speed

Gear	Times	Time/s	Average time/s	Driving speed / (m·s^{-1})
Slow gear	1	200.69	198.79	0.25
	2	197.23		
	3	198.46		
Medium gear	1	105.16	105.44	0.47
	2	103.83		
	3	107.33		
Fast gear	1	62.36	63.37	0.79
	2	64.28		
	3	63.47		

As can be seen from Table 2, the driving speeds of the tobacco harvester at different gear settings are 0.25 m/s, 0.47 m/s, and 0.79 m/s, respectively, with the maximum driving speed being close to the predetermined target speed (3 km/h).

The machine is capable of driving at medium to high speeds in the field or on the road. Due to the power loss of the entire machine and the slippage of the track chassis on the field road surface (*Wu et al., 2024*), the actual driving speed is slightly lower than the target speed.

Steering Test

The turning performance of the chassis is characterized by the turning radius. During the steering process, the maximum circular radius drawn by the track on the ground is the turning radius. When the steering wheel is fully turned to the left or right, the rotation angles of the two flow control valves of the series piston pump are the same but opposite in direction, causing the tracks to move at the same speed but in opposite directions, thus achieving the pivot turn of the tobacco harvester chassis. According to the standard GB/T 3871.5-2006 “Steering Circle and Passing Circle Diameter”, the turning radius test was conducted on an open area of the processing plant. During the test, the machine was driven in slow gear, then the steering wheel was turned fully to the left or right, the machine rotated 360 degrees and the steering wheel was returned to the center, and then driven out of the test area. The diameters at the 0, 120, and 240-degree positions of the turning circle were measured, and the mean value and minimum turning radius were calculated. The test process is shown in Figure 9 (b), and the test results are shown in Table 3.

Table 3

Test results for minimum turning radius

Steering direction	Measurement location	Diameter/mm	Mean Diameter/mm	Turning radius/mm
Left turn	0°	1593	1552	776
	120°	1566		
	240°	1496		
Right turn	0°	1483	1532	766
	120°	1536		
	240°	1576		

As can be seen from Table 3, the minimum turning radius of the whole machine is 766 mm, which meets the design requirements for tobacco leaf operation and transfer. Compared with the track gauge, the measured value is slightly larger, mainly due to the overall weight of the machine and the presence of certain track slip and skid during turning.

Field experiment

To further verify the agronomic compatibility of the chassis, field harvesting trials were conducted at a tobacco planting base in Chenzhou, Hunan Province, as shown in Figure 10.

Fig. 10 - Field harvesting experiment

The experimental results indicate that the tobacco harvester operates smoothly with sufficient power. The failure rates for tobacco stalk clamping on three rows of tobacco were 4.91%, 3.38%, and 4.83% respectively, with a low overall clamping failure rate. The chassis has good agronomic compatibility and can complete the tobacco harvesting task relatively smoothly.

For the cases of tobacco stalk clamping failure, the analysis suggests that the cause may be related to the tobacco stalks being deeply rooted in the soil, which leads to the chisel-shaped spade of the soil loosening mechanism failing to effectively lift the stalks out of the soil. This affects the normal conveyance of the clamping chain, resulting in clamping failure. To further improve the success rate of clamping, subsequent optimizations to the design of the soil loosening mechanism will be made, enhancing the penetration power and soil adaptability of the spade head to ensure effective digging and clamping of tobacco stalks under various soil conditions. This will improve overall operational efficiency and the quality of tobacco leaf harvesting.

CONCLUSIONS

(1) To address the issues of difficult control and easy dislocation of control levers when tracked vehicles turn while traveling, this paper designs a tobacco harvester hydraulic drive chassis based on steering wheel control. This design can solve the problems of insufficient accuracy and complex operation inherent in traditional control methods. Through the design of the chassis structure and the selection of key components, and the performance test of the prototype, its applicability in tobacco harvesting has been verified.

(2) The chassis adopts a hydraulic drive system, with a power of 31 kW and a tracked drive mode. A steering strategy for straight steering control with the steering wheel is proposed, by adjusting the opening of the flow control valve of the series variable plunger pump, thus achieving control over the speed of the left and right tracks.

(3) The test results show that the tobacco harvester chassis can achieve three-speed gear shifting in actual work, with the highest travel speeds of 0.25 m/s, 0.47 m/s, and 0.79 m/s respectively, meeting different travel speed requirements; the minimum turning radius is 766 mm; field harvesting test results show that the machine runs smoothly during operation, the power system is sufficient, and can effectively cope with complex terrain and irregular crop planting environments. The average tobacco rod clamping failure rate is 4.37%, with a low overall clamping failure rate, meeting the requirements of field operations.

ACKNOWLEDGEMENT

Funding: This study was supported by the scientific research business fee fund (HN2023KJ06) of China National Tobacco Corporation Hunan Provincial Company.

REFERENCES

[1] Chen Z., Guo X., Zhang C. (2010). The effect of the design of the ground aspect ratio on the driving performance of crawler vehicles [J]. *Research of Agricultural Mechanization*, 32(05): 112-4.

[2] Ding Z., Li Y, Tang Z. (2020). Analysis of the compaction effect of wheeled and crawler vehicles on farmland soil [J]. *Transactions of the CSAE*, 36(05): 10-8.

[3] Du X., Ning C., Yang Z., Ma C., He L., Han X. (2023). Design and Experiment of the Crawler Chassis Walking Hydraulic System for a Straddle-type Camellia Fruit Harvester [J]. *Transactions of the Chinese Society for Agricultural Machinery*, 54(03): 139-47.

[4] Li M., Yang Q., Xie K., Wang Y., Xu D., Zhang Z. (2024). Design and experimental study on the hydraulic system of a self-propelled notoginseng combined harvester [J]. *Journal of Engineering Design*, 31(05): 670-80.

[5] Li S., Chen H., Peng J., Men L., Zhang X., Li M. (2024). Design and test of a full hydraulic remote-controlled crawler power chassis for hilly and mountainous orchards [J]. *Transactions of the Chinese Society for Agricultural Machinery*, 55(02): 119-27+201.

[6] Liu C., Li J., Wang H., Peng Z., Duan M., He W. (2024). Current situation and countermeasure analysis of tobacco leaf mechanical harvesting development [J]. *Southern Agricultural Machinery*, 55(10): 24-8+32.

[7] Liu F. (2022). *Optimization of the crawler self-propelled potato harvester chassis* [D], Huazhong Agricultural University.

[8] Li Q., Sun Z., Ren Q., Guo H., Zhang C., Luo S. (2024). Design and test of a self-propelled garlic harvester with continuous laying [J]. *Chinese Journal of Agricultural Mechanization*, 45(09): 1-7+14.

[9] Mei S., Tang D., Shi Z., Song Z., Tian C., Zhou R. (2024). Design and test of the goji berry harvester based on arrayed vibration units [J]. *Transactions of the CSAE*, 40(23): 115-25.

[10] Pan J., Xu L., Lu E., Dai B., Chen T., Sun W. (2024). Design and Experiment of an Unoccupied Control System for a Tracked Grain Vehicle [J]. *Sensors*, 24(9):2715. https://www.mdpi.com/1424-8220/24/9/2715

[11] Tan S., Sun C., Li J., Xiao M., Ai W., Liu H. (2023). Current situation and countermeasure research on tobacco leaf mechanized harvesting in southern hilly areas [J]. *Southern Agricultural Machinery*, 54(14): 33-6.

[12] Wang B., Zhu J., Chai X., Liu B., Zhang G., Yao W. (2024). Research status and development trend of key technology of agricultural machinery chassis in hilly and mountainous areas [J]. *Computers and Electronics in Agriculture*, 226: 109447.

[13] Wang D., Zhao Y., You Y., Zhang X., Wang T., Li S. (2023). Design and test of the crawler self-propelled gentle slope grass harvester chassis [J]. *Transactions of the Chinese Society for Agricultural Machinery*, 54(09): 178-87.

[14] Wang P., Yi W., Xiong C., Cheng F., Deng J., Zhou Y. (2022). Design and test of the 4CJZ-1000 self-propelled tea harvester [J]. *Journal of Southwest University (Natural Science Edition)*, 44(11): 228-33.

[15] Wu L., Dong S., Liu T., Yahg J., Yan X. (2018). Design and test of a self-propelled sweet sorghum harvesting and spreading machine [J]. *Agricultural Engineering*, 8(10): 90-4.

[16] Wu P., Sun W., Wang H. (2024). Design and Testing of an Inter-Toothed, Self-Propelled Digger for Deep-Rhizome Chinese Herbal Medicines [J]. *Agronomy*, 14(9):2024.

[17] Wu Z., Chen L., Wang Y., Luo K., Lai X., Zhang X. (2024). Design and test of the track self-propelled tea harvester walking chassis passability [J]. *Transactions of the Chinese Society for Agricultural Machinery*, 56(01):474-483.

[18] Xi C., Zhang F., Zheng L., Han Z., He C. (2024). Research on the design and collaborative control of the hydraulic system of agricultural power chassis in hilly and mountainous areas [J]. *Machine Tools and Hydraulics*, 52(20): 35-41.

[19] Xiao M., Zhao Y., Wang H., Xu X., Zhu Y. (2024). Design and Test of Hydraulic Driving System for Undercarriage of Paddy Field Weeder [J]. *Agriculture*, 14(4):595.

[20] Xiao W., Tong J. (2023). Design of the hydraulic drive system of the crawler tractor [J]. *Research of Agricultural Mechanization*, 45(11): 253-8.

[21] Xue B., Li J., Jiao W., Li H., Liu X. (2024). Current situation and development trend of tobacco agricultural machinery and agronomy integration [J]. *Agricultural Equipment and Vehicle Engineering*, 62(02): 29-33.

[22] Zhou Y., Wu J., Lin C., Deng J. (2024). Current situation and development suggestions of tobacco mechanization research in hilly and mountainous areas [J]. *Sichuan Agricultural Science and Technology*, (10): 121-5+39.